Journal of Guidance, Control, and Dynamics
Vol. 29, No. 6, November–December 2006

Engineering Notes

ENGINEERING NOTES are short manuscripts describing new developments or important results of a preliminary nature. These Notes should not exceed 2500 words (where a figure or table counts as 200 words). Following informal review by the Editors, they may be published within a few months of the date of receipt. Style requirements are the same as for regular contributions (see inside back cover).

Collision Probability for Larger Bodies Having Nonlinear Relative Motion

Russell P. Patera*
The Aerospace Corporation, Los Angeles, California 90009-2957

DOI: 10.2514/1.23509

Nomenclature

d	=	cross-sectional radius of torus
$\mathrm{d}z$	=	subvolume height
h	=	distance above x–y plane of torus
P	=	collision probability
P_R	=	collision probability rate
R	=	radius of torus
r	=	polar coordinate in symmetrized encounter plane
t	=	time
V_z	=	in-track velocity in symmetrized encounter frame
x, y, z	=	coordinates used in probability density function
θ	=	contour integration parameter
ρ	=	three-dimensional probability density function
σ	=	standard deviation in symmetrized encounter frame
$\sigma_{x,y,z}$	=	standard deviations of relative position uncertainty for each axis in diagonal frame

Introduction

MOST encounters between orbiting space objects are at high relative velocity, on the order of thousands of meters per second. This is due to the high velocity required to attain orbit and the differences in the orbits themselves. Most collision probability calculation methods assume that the relative velocity between the objects is high enough and that the relative trajectory traces a straight line. This linear motion assumption is valid in nearly all encounters. Nevertheless, some satellite encounters in the geosynchronous Earth orbit (GEO) belt and encounters between satellites in nearly the same circular orbit exhibit relative trajectories that trace curved paths. These nonlinear relative motion cases require special attention when computing collision probability.

Fortunately, a method has been developed to compute collision probability for space objects having nonlinear relative motion [1–5]. It has been implemented in the nonlinear collision probability tool (NCPT) and validated with cases having known results [1]. In addition, a real-world case has been validated using a Monte Carlo simulation [1]. There are several very useful features of the nonlinear collision probability method:

1) It uses the same input as the linear collision probability method referred to as the collision probability tool (CPT).
2) It can account for time-varying position error throughout the encounter.
3) It can account for the time-varying hardbody collision area that is defined by the physical size of the of the space objects.
4) It is applicable to asymmetric hardbody shapes.

Like CPT, NCPT is valid for all combined hardbody sizes when the relative motion is linear. However, if the relative motion is nonlinear and the combined hardbody size is nearly equal to the standard deviation, a small error can result, as was reported earlier [1–4]. The current work seeks to extend the validity of NCPT to larger values of hardbody sizes and position uncertainty. This is achieved by more accurately evaluating the probability increments associated with trajectory segments, as illustrated in Fig. 1. A probability increment is the probability density at the location of the trajectory segment times the volume of the segment. Each segment in Fig. 1 is divided into smaller volumes to evaluate probability increments more accurately. The increments are summed to yield the total collision probability.

The refined method was tested with special cases having known values of collision probability. Some of the known values were obtained via a specialized computer simulation that was developed based on an alternative method, referred to as NCPT-A, that integrates through the volume linearly in a direction normal to the relative velocity, thereby avoiding nonlinear motion concerns. Comparisons of the results indicate that NCPT accurately computes collision probability.

Analysis

The first step in computing collision probability for nonlinear relative motion is to transform the problem to a symmetrized frame in which the position uncertainty is spherically symmetric. Finding the principal axes of the position-error ellipsoid and performing a scale change along two of the principal axes achieves this transformation. The magnitude of each scale change is selected to make its associated position-error standard deviations equal to that of the third principal axis. The position-error ellipsoid becomes spherical in the symmetrized frame. The scale changes needed for the symmetrization are applied to state vectors and points defining the combined hardbody boundary. The collision probability is found by integrating the relative position probability density over the volume swept out by the combined hardbody of two space objects.

$$P = \iiint_{\mathrm{vol}} \rho(\boldsymbol{x})\,\mathrm{d}x\,\mathrm{d}y\,\mathrm{d}z \tag{1}$$

The uncertainty in the relative position between the objects is defined by a three-dimensional Gaussian distribution of the form

$$\rho(\boldsymbol{x}) = \frac{(2\pi)^{-3/2}}{\sigma_x\sigma_y\sigma_z}\exp\left[\left(\frac{-x^2}{2\sigma_x^2}\right) + \left(\frac{-y^2}{2\sigma_y^2}\right) + \left(\frac{-z^2}{2\sigma_z^2}\right)\right] \tag{2}$$

Here, the probability density is represented in the diagonal frame of the position-error covariance matrix. The difficulty in evaluating Eq. (1) is in defining the volume of integration. Therefore, scale changes on two of the three axes are performed to symmetrize the

Presented at the AAS/AIAA Astrodynamics Specialists Conference, Lake Tahoe, California, 7–11 August 2005; received 27 February 2006; revision received 19 June 2006; accepted for publication 6 July 2006.

*Senior Engineering Specialist, Center for Orbital and Reentry Debris Studies, Mail Stop M4-066.

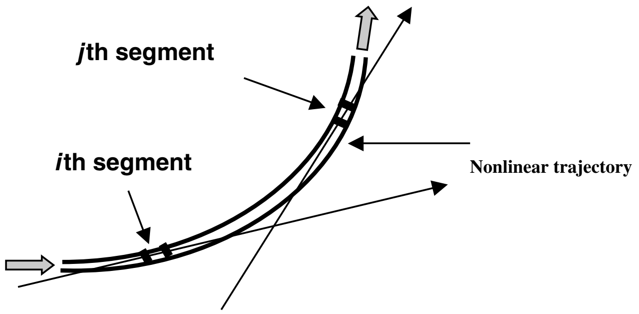

Fig. 1 Nonlinear trajectory and associated integration volume in the symmetrized frame.

problem. In the symmetrized frame, the probability becomes

$$P = \left[\frac{1}{\sqrt{2\pi}\sigma}\int_{-\infty}^{\infty}\exp\left(\frac{-z^2}{2\sigma^2}\right)\mathrm{d}z\right] \times \left(\frac{1}{2\pi}\right)\oint_{\text{perimeter}}\left[1-\exp\left(\frac{-r^2}{2\sigma^2}\right)\right]\mathrm{d}\theta \tag{3}$$

where the x, y integration was simplified to a one-dimensional contour integration about the hardbody area in the symmetrized encounter plane. Further simplification can reduce the contour integral to a definite integral [6]. The incremental probability associated with each trajectory segment illustrated in Fig. 1 can be defined as

$$P_I = \left[\frac{\mathrm{d}z}{\sqrt{2\pi}\sigma}\right]\exp\left(\frac{-z^2}{2\sigma^2}\right)\left(\frac{1}{2\pi}\right)\oint_{\text{perimeter}}\left[1-\exp\left(\frac{-r^2}{2\sigma^2}\right)\right]\mathrm{d}\theta \tag{4}$$

The probability rate can be defined as

$$P_R = \left[\frac{V_z}{\sqrt{2\pi}\sigma}\right]\exp\left(\frac{-z^2}{2\sigma^2}\right)\left(\frac{1}{2\pi}\right)\oint_{\text{perimeter}}\left[1-\exp\left(\frac{-r^2}{2\sigma^2}\right)\right]\mathrm{d}\theta \tag{5}$$

The collision probability rate is integrated over the time of interest to obtain the total collision probability associated with the time interval from t_1 to t_2.

$$P = \int_{t_1}^{t_2} P_R(t)\,\mathrm{d}t \tag{6}$$

Because the velocity direction changes from volume increment to volume increment, there are overlaps and gaps between adjacent volumes. Because volumes associated with the overlaps and gaps are nearly equal, the associated probabilities tend to compensate, especially if the probability density is fairly uniform throughout the incremental volume. The residual error is small as long as the hardbody is significantly smaller than the position-error ellipsoid, which is the situation in very nearly all real cases.

One method to reduce the overlaps and gaps is to account for the changes in the velocity direction from incremental volume to incremental volume. This is accomplished by dividing each incremental volume into smaller volumes. As a result, the contour integration is divided into smaller contours associated with each area, as illustrated in Fig. 2. The height of each volume is adjusted by the change in velocity direction, as illustrated in Fig. 3. Each smaller volume has a unique probability rate. The probability rates are summed to obtain the total probability for each increment. This process is repeated for each trajectory increment. Finally, the probability rates were integrated over the time of interest in Eq. (6).

The number of segments can be adjusted to obtain the desired accuracy. Five radial segments and 20 angular segments were found to be adequate for all cases examined. The additional computational cost was not a problem, because of the tremendous numerical efficiency of the contour integration method.

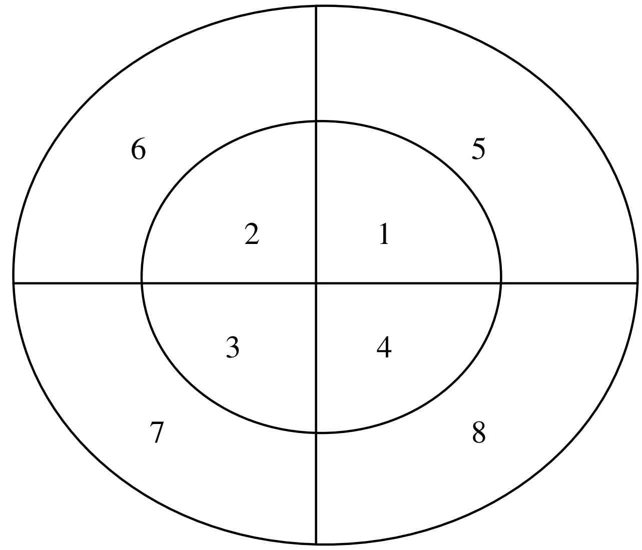

Fig. 2 Cross section of incremental volume, illustrating division into eight smaller volumes.

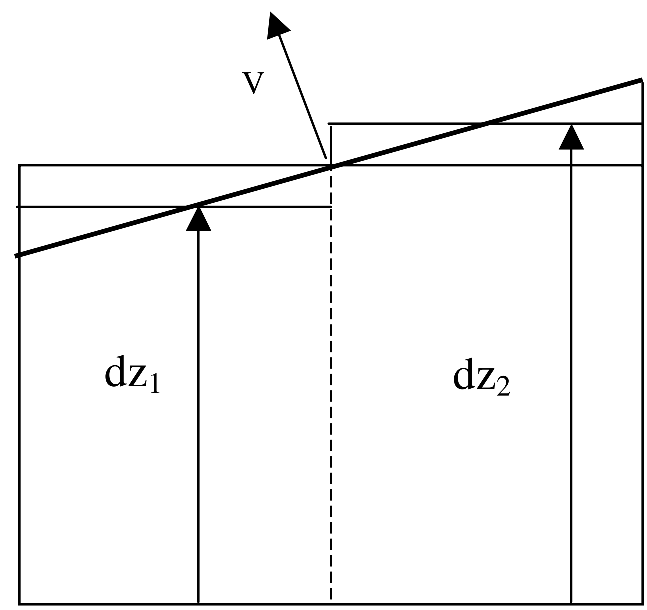

Fig. 3 Subvolume heights $\mathrm{d}z_1$ and $\mathrm{d}z_2$, associated with change in velocity direction.

Numerical Results

A toroidal volume was used for a test case, because it has a simple solution involving only a simple integral [1]. The torus was placed a distance h above the x–y plane, as illustrated in Fig. 4. The axis of the torus was aligned with the z axis. The radius of the torus and the radius of its cross section are denoted R and d, respectively. The position-error standard deviation along the z axis differs from that along the x and y axes, σ. The probability associated with an object sweeping through the toroidal-shaped volume can be reduced to a simple integral given by

$$P = \sigma_z^{-1}\sqrt{\frac{2}{\pi}}\exp\left[\frac{h^2}{2\sigma^2}-\frac{(R^2+d^2)}{2\sigma^2}\right]\int_{h-d}^{h+d}\exp\left[\frac{-z^2}{2}\left(\frac{1}{\sigma_z^2}-\frac{1}{\sigma^2}\right)-\frac{zh}{\sigma^2}\right]\sinh\left[\frac{R\sqrt{d^2-(z-h)^2}}{\sigma^2}\right]\mathrm{d}z \tag{7}$$

The equation reduces to the equation derived earlier [1] when $h=0$ and $\sigma_z=\sigma$. Equation (7) was implemented in a computer program

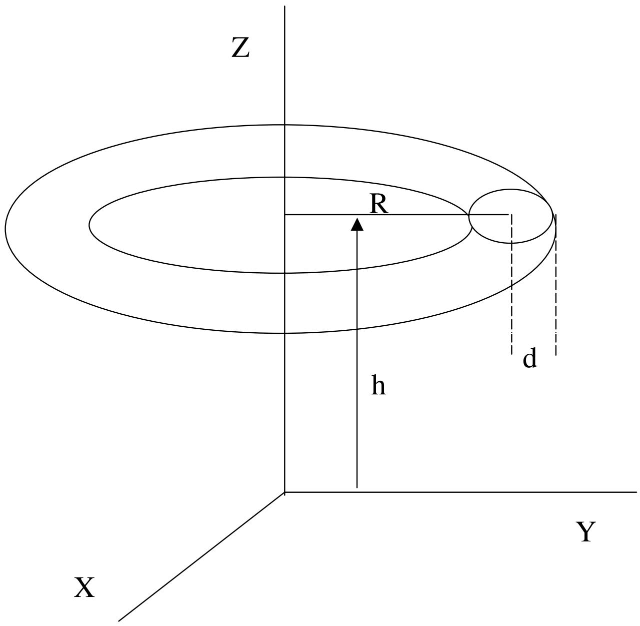

Fig. 4 Toroidal volume with axis aligned, with the z axis centered a distance *h* above the x–y plane.

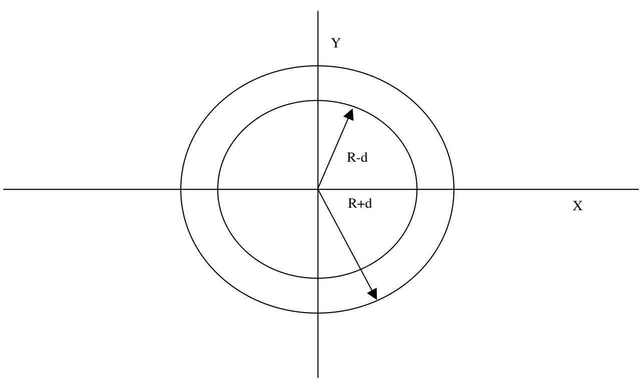

Fig. 5 Annular integration area in the encounter plane for $z = h$, used in NCPT-A.

and results were compared with those of NCPT. Two methods of employing NCPT on this case were used. The first method of using NCPT (NCPT-A) is to simply sweep along the z axis so that the encounter plane is the x–y plane. In this case, the hardbody area in the encounter plane varies with time.

Figure 5 illustrates the shape of the hardbody area for $z = h$. The hardbody area is zero for $z < h - d$, but begins to increase for $z > h - d$. The annular region increases until $z = h$, as shown in Fig. 5. As z increases beyond h, the annular region shrinks until it is zero at $z = h + d$. The area remains zero for $z > h + d$. This method also demonstrates the ability of NCPT to treat time-varying hardbody shapes.

The second method of using NCPT (NCPT-B) is to sweep through space in the direction of the relative velocity vector; that is, in a circle of R about the axis of the torus. In effect, the hardbody carves out the toroidal volume. This method offers more flexibility, because the volume swept out can be arbitrarily shaped depending on the time-varying relative velocity. This approach provides a very good approximation to the exact solution.

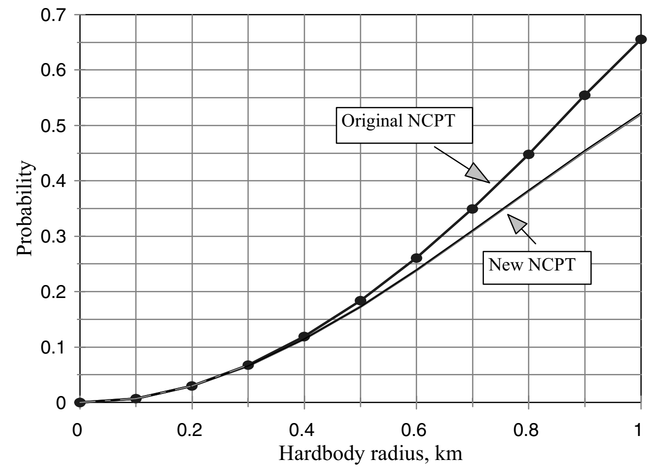

Fig. 6 Comparison of results for larger hardbody sizes.

Figure 6 illustrates the collision probability for $R = 1$ km, $\sigma = 1$ km, and $h = 0$ for various values of d. Numerical integration of Eq. (7) provides the correct result. Both NCPT-A and NCPT-B were used and gave the correct result, as presented in Table 1. Results for the original version NCPT, which is not valid for these larger hardbody sizes, is also illustrated in Fig. 6 and Table 1. Notice that the original versions provided the correct result in its region of validity; that is, smaller hardbody sizes.

Figure 7 illustrates results for various values of standard deviation along the z axis, keeping x axis and y axis standard deviations and R fixed at 1 km. Once again, both NCPT-A and NCPT-B yielded correct results.

When the torus is moved above the x–y plane, the collision probability for $R = 1$ km and $\sigma = 1$ km is reduced, as illustrated in Fig. 8. Both NCPT methods yielded correct results.

If σ_x differs from σ_y, Eq. (7) is no longer valid. Nevertheless, the collision probability can be obtained using NCPT. Figure 9 illustrated results using both NCPT methods for a hardbody radius of 1 km. Sweeping through the volume along the z axis (NCPT-A) provides the correct result, whereas sweeping around the toroidal volume (NCPT-B) introduces a small, but acceptable, amount of error. Figure 10 presents results for a hardbody radius of 0.6 km.

Sweeping through the volume in the direction of the relative velocity direction provides a versatile computation method. The relative trajectory can be arbitrary, both the integration region and position-error standard deviation can be time-varying. This is due to the fact that probability rates and associated probability increments are independent.

Another check of the new version of NCPT was performed using actual space vehicle data for a case involving nonlinear relative motion. Figure 11 illustrates results from NCPT and relative separation distance. Also illustrated in Fig. 11 is the collision probability computed at each instant of time using CPT. At the reported point of closest approach, the collision probability from CPT is 6.55×10^{-7}. Even at the actual point of closest approach, the collision probability from CPT is only 1.7×10^{-6}. The correct collision probability for the encounter is 3.16×10^{-6}, which is obtained by both old and new versions of NCPT. For most cases, the original version of NCPT is adequate to obtain the correct result,

Table 1 Summary of results

Hardbody radius, km	0.1	0.2	0.3	0.4	0.5	0.6	0.7	0.8	0.9
Exact	7.57e − 3	2.99e − 2	6.61e − 2	1.15e − 1	0.173	0.239	0.310	0.382	0.454
NCPT-A	7.57e − 3	2.99e − 2	6.61e − 2	1.15e − 1	0.173	0.239	0.310	0.382	0.454
NCPT-B	7.56e − 3	2.99e − 2	6.61e − 2	1.15e − 1	0.173	0.239	0.310	0.383	0.455
Original NCPT	7.58e − 3	3.02e − 2	6.76e − 2	1.19e − 1	0.184	0.261	0.350	0.448	0.555

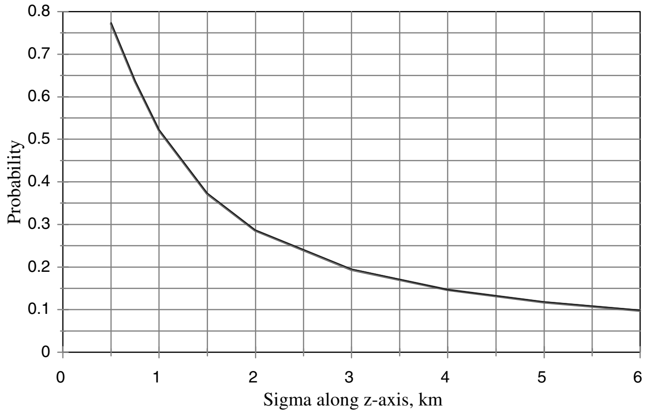

Fig. 7 Probability as a function of z-axis position-error standard deviation.

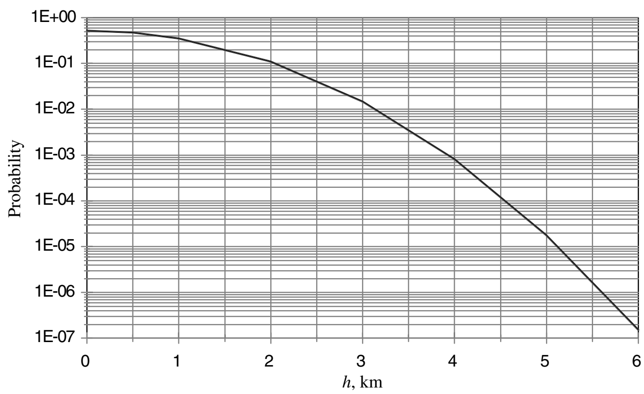

Fig. 8 Probability vs torus height above the x–y plane.

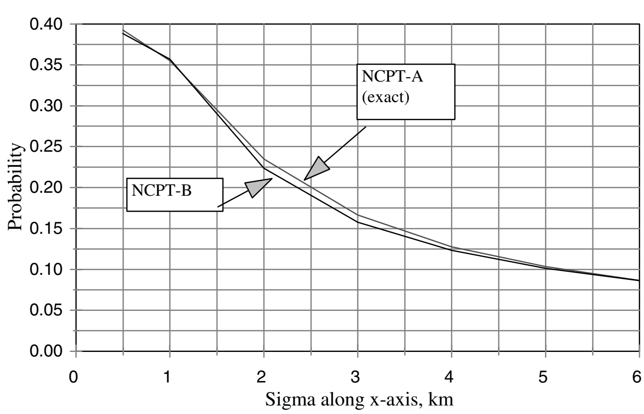

Fig. 9 Probability vs x-axis standard deviation for a hardbody radius of 1 km.

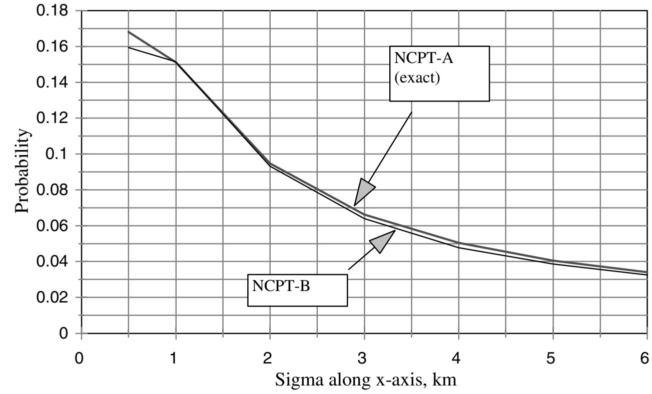

Fig. 10 Probability vs x-axis standard deviation for a hardbody radius of 0.6 km.

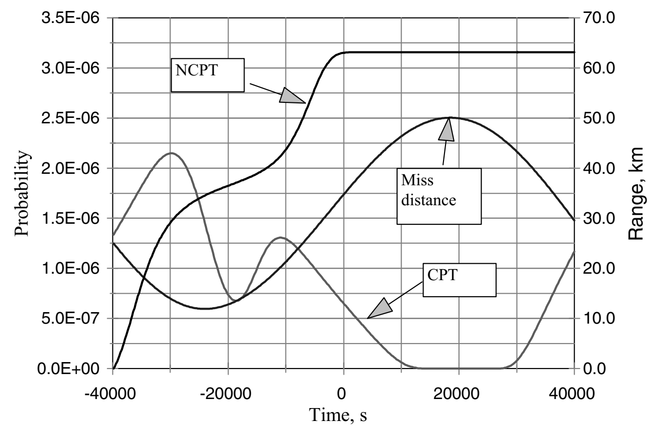

Fig. 11 Comparison of collision probabilities obtained with CPT and NCPT for nonlinear relative motion.

because they involve hardbody sizes less than the position-error standard deviation.

The new version of NCPT should be used when the hardbody size is significant relative to the position uncertainty standard deviation. If computational effort is not a concern, the new version of NCPT could be used in all cases, but, otherwise, employed judiciously.

Conclusions

A method to compute collision probability between two space objects whose relative motion is not linear was developed and implemented in NCPT. For cases having hardbody sizes comparable to the position-error standard deviation, each in-track trajectory volume increment was divided into smaller volumes, to maintain accuracy. The smaller volumes more accurately account for the twisting of each in-track trajectory volume increment due to changing velocity direction. The method was stress-tested with a circular trajectory test case having a known collision probability and correct results were obtained. Asymmetric stress test cases were also tested and provided acceptable results.

Acknowledgments

The author would like to thank William Ailor, Vladimir Chobotov, and Charles Gray for reviewing this paper and providing very useful suggestions to improve it.

References

[1] Patera, R. P., "Satellite Collision Probability for Non-Linear Relative Motion," AIAA Paper 2002-4632, 2002.
[2] Patera, R. P., "Application of Symmetrized Covariances in Space Confliction Prediction," Committee on Space Research (COSPAR), Paper PEDAS1-B1.4-003902, 2002.
[3] Patera, R. P., "Contour Integration Method for Space Vehicle Interference Prediction," *Satellite Operations and Safety Workshop '04*, Massachusetts Inst. of Technology, Lincoln Lab., Lexington, MA, Oct. 2004.
[4] Patera, R. P., "Satellite Collision Probability for Non-Linear Relative Motion," *Journal of Guidance, Control, and Dynamics*, Vol. 26, No. 5, Sept.–Oct. 2003, pp. 728–733.
[5] Patera, R. P., "Application of Symmetrized Covariances in Space Confliction Prediction," *Advances in Space Research*, Vol. 34, No. 5, 2004, pp. 1115–1119.
[6] Patera, R. P., "Convention Form of the Collision Probability Integral for Arbitrary Space Vehicle Shape," AIAA Paper 2004-5218, 2004.